CRITICAL STATE FRAMEWORK AND LIQUEFACTION OF FINE-GRAINED SOILS

By

DIANA WORTHEN

A thesis submitted in partial fulfillment of
the requirements for the degree of

MASTER OF SCIENCE IN CIVIL ENGINEERING

WASHINGTON STATE UNIVERSITY
Department of Civil and Environmental Engineering

AUGUST 2009

To the Faculty of Washington State University:

The members of the Committee appointed to examine the thesis of DIANA WORTHEN find it satisfactory and recommend that it be accepted.

_____

Balasingam Muhunthan, Ph.D., Chair

_____

William F. Cofer, Ph.D.

_____

Haifang Wen, Ph.D.

ACKNOWLEDGEMENT

First I would like to thank my advisor, Dr Balasingam Muhunthan. He guided and supported my academic success with a generous dedication beyond expectation. I will be forever grateful for his taking a personal interest in my career. I always appreciate the extraordinary knowledge he imparts so clearly and patiently, the calculated challenges he imposes to make his students stretch, and especially his welcoming open friendship.

Thank you to Dr David McLean, Dr Adrian Rodriguez-Marek, and Dr Mike Wolcott for their gracious patience and understanding while I found my path. I was lucky to find their support when I really needed it. Thank you also to Dr William Cofer and Dr Haifang Wen for granting me your confidence and endorsement and serving as my committee.

I owe a special thanks to the Department of Civil and Environmental Engineering of Washington State University for its financial support of my studies. Its generosity has helped me achieve my academic goals at this exceptional institution.

Thank you to Vicki Ruddick, Brooke Whiting, Maureen Clausen, and Glenda Rogers for always happily solving my problems. Thanks to all of my students for never complaining when class ran late (again). Much warm gratitude goes to my friends and colleagues for many late nights of solving impossible homework problems and a few more evenings of unscholarly but much-needed diversions. In particular, without the encouragement, ever-sympathetic ears, inspiration, and ready laughs of Steven Greenwood, Tony Cameron, and Amy Jo Hendershot, I would never have arrived at this point in my journey.

Finally, thank you to my parents for instilling in me a respect and need for education from my very start.

CRITICAL STATE FRAMEWORK AND LIQUEFACTION

OF FINE-GRAINED SOILS

Abstract

By Diana Worthen, M. S.
Washington State University
August 2009

Chair: Balasingam Muhunthan

This study is on the characterization of the liquefaction potential of fine-grained soils, which is currently evaluated based on plasticity characteristics using the 'Chinese criteria.' Recent research shows that such criteria are ineffective. In addition, the current liquefaction models do not account for the confining pressure of in-situ soil or the strength of the earthquake.

This study uses the critical state soil mechanics framework, which emphasizes that the shear strength and deformation behavior of soil depends on changes in volume and confining stress. Depending on their combination, a soil aggregate may fracture into clastic debris, fail with fault planes, or yield plastically.

The central piece of the proposed characterization of soil behavior is the (η, LI_5) stability diagram where $\eta = q / p'$ and $LI_5 = LI + 0.5 \log (p'/5)$. This diagram captures the effects of soil plasticity through LI, confinement through mean normal effective stress p', and shear stress q through the stress ratio η. The three regions of behavior; fracture, fault, and fold/yield, are identified using the Weald clay data. Soils become susceptible to

liquefaction when they shift above the $\eta = 1$ line in the fracture zone ($LI_5 \leq 0.4$), or if they plot outside of the cam clay region.

The proposed characterization of soil behavior is used to examine the liquefaction susceptibility of fine-grained soils from China, Taiwan, and Turkey. First the equivalent liquidity LI_5 and shear stress ratio η are determined. Changes in these parameters due to earthquake magnitude M_w, peak ground acceleration a_{max}, and pore pressure rise are determined. It is shown that the critical state soil mechanics framework provides a consistent characterization of liquefaction susceptibility with the inclusion of depth and earthquake load in addition to soil plasticity characteristics.

The analyses show that upwards shifts in η or larger shifts in LI_5, make a soil more likely to liquefy. A higher a_{max} value increases η. A greater depth below ground surface decreases η. A larger earthquake magnitude causes a larger shift in LI_5. Many soils that at rest plot outside of the cam clay region remain stable due to natural cementation. However, these sensitive bonds can be broken under earthquake loads, leading to unstable failures.

TABLE OF CONTENTS

LIST OF FIGURES

CHAPTER 1
INTRODUCTION

Background

The liquefaction of soils causes some of the most serious structural damage during an earthquake. It is a complex problem on which a great deal of research has been done. Much of the research done has involved the liquefaction of sands. However, many earthquake-induced ground failures have occurred in sites containing fine-grained soils (silts and clays). Such soils are often found beneath critical infrastructures. Thus, methods that could predict conditions that would lead to the liquefaction of such fine grained soils are needed. Liquefaction potential of fine-grained soils is currently evaluated by the 'Chinese criteria,' based on their plasticity characteristics, introduced by Dr. Wang Henshao in 1979 based on the study of major earthquakes in China. They were expanded by Seed and Idriss in 1982 and became the commonly accepted method for predicting fine-grained liquefaction susceptibility. More recent research by Boulanger and Idriss (2006) and Bray and Sancio (2006) have shown that the Chinese criteria are ineffective and should not be relied upon to safely predict liquefaction potential. They have proposed modifications to the Chinese criteria for predicting the liquefaction potential of fine grained soils. None of these criteria, however, account for the effects of confining pressure of in-situ soil.

It is now known that the shear strength and deformation behavior of soil is very sensitive to the combination of changes in volume and the confining stress. Depending on their combination, a soil aggregate may fracture and crack into clastic debris, or fail with fault planes on which gouge material dilates and softens, or it can continue to yield and deform plastically. The current liquefaction models can not distinguish between these distinct classes of soil

behavior and have led to many of the difficulties researchers are faced with the interpretation of liquefaction failures.

Critical state soil mechanics (CSSM), developed in the 1960's, explicitly recognizes that soil is an aggregate of interlocking frictional particles and that the regimes of soil behavior depend in a major way on its density and effective pressure. Detailed accounts of the basic principles of the CSSM framework have been presented in a number of publications including a classical text by Schofield and Wroth (1968). A succinct account of this strength representation and applications of the critical state framework to geotechnical practice is presented in the new book by Schofield (2005).

This study makes use of the CSSM framework to propose a consistent methodology to predict the liquefaction potential of fine-grained soils.

Objectives

The specific objectives of this study are to:

1. document and examine the performance of fine-grained soils under cyclic loading.
2. develop a criteria for liquefaction potential for fine-grained soils based on the critical state framework, and
3. apply the new framework to the field prediction of the liquefaction of fine-grained soils.

Organization of Thesis

This thesis is organized into five chapters.

Chapter 2 discusses how we define liquefaction and provides a literature review of basic methods of liquefaction analysis in field studies, with a focus on fine-grained soils. Our

understanding of liquefaction is constantly being revised as new evidence is discovered and studied. As studies continue, the ability to predict the likelihood of a soil to liquefy is improving, especially for fine-grained soils.

Chapter 3 provides an overview of critical state soil mechanics and describes the critical state view of the liquefaction of fine-grained soils. It discusses the different classes of soil behavior as a combination of void ratio and confining stress. The state of stress of a soil in this framework is described by three parameters: the mean normal effective stress, the shear stress, and the void ratio or specific volume. With normalization, the framework can be represented in two dimensions. The axes of this normalized stress framework are converted to equivalent liquidity which enables the examination of the effect of plasticity characteristics on soil behavior. Liquefaction potential can be determined by where the state of stress of a soil plots with relation to the failure curve.

Chapter 4 shows the analysis of the data with respect to critical state soil mechanics. Data is used from field studies of the liquefaction of fine-grained soils and from the original development of the Chinese criteria. The field study data is used to compare the Chinese criteria assessment method to that of the critical state framework. The effect of two significant parameters (peak ground acceleration, a_{max}, and depth) on the shift of the stress ratio, η, under an earthquake load is analyzed. Finally, the impact of cementation bonding on liquefaction of sensitive clays is considered.

Chapter 5 gives conclusions drawn from the study and recommendations for future study of fine-grained soil liquefaction.

CHAPTER 2
LIQUEFACTION ANALYSIS

General

This chapter discusses the various definitions of liquefaction and provides a literature review of basic methods of liquefaction analysis in field studies, with a focus on fine-grained soils. Our understanding of liquefaction is constantly being revised as new evidence is discovered and studied. As studies continue, the ability to predict the likelihood of a soil to liquefy is improving, especially for fine-grained soils.

Liquefaction of Sands

The liquefaction of loose, saturated sands has been studied extensively and currently is relatively well understood. Under cyclic loading, such as an earthquake, the soil particles have a tendency to rearrange and densify, much as a glass of ice cubes will pack down when shaken. As the particles attempt to densify, the in-situ stress carried by the mineral skeleton is transferred to the incompressible pore water trapped in the voids. It cannot escape the soil quickly enough as the voids try to collapse. Thus, the pore water takes on the load from the particles, resulting in a load increase. As pore water pressure increases, effective confining pressure decreases, leading to a significant loss of shear strength as the particles lose contact with each other. This phenomenon causes significant damage to the structures above that rely on soil for support. Such failures include overturning of buildings and complete 'washouts' of roads, as was particularly evident in the 1964 earthquakes in Anchorage, Alaska and Nigatta in Japan.

Information on liquefaction behavior of silts and clays of low plasticity is not as readily available. Ishihara et al (1975, 1981) conducted experimental investigations to determine the

behavior of mine tailings having clay fines. These studies showed that clays of low plasticity exhibit potential for large deformation even though liquefaction, as defined by pore water pressure becoming equal to initial effective confining pressure, may not occur. Recent earthquakes have shown abundant evidence of large deformation associated with fine-grained soil liquefaction. Figure 2-1 shows examples of building damage that resulted from such fine-grained soil liquefaction in Adapazari, Turkey in the 1999 Kocaeli earthquake.

Figure 2-1. Liquefaction failures of silts in Adapazari, Turkey (Bray and Sancio 2006)

The behavior of fine-grained soils under cyclic loading is not as well understood as sands. They are more difficult to study since reconstituted samples poorly represent the behavior of in-situ soil, which is greatly affected by its structure. In addition, the structure of different types of fine-grained soils varies widely.

The term liquefaction, indicating what occurs when pore water pressure becomes equal to initial effective confining pressure, is widely used in the geotechnical literature. It has its origin in its usage by Hazen (1920) in the context of hydraulic–fill dam failures. However, large deformations associated with the liquefaction of silts, even though the pore water pressure is below the initial effective confining pressure, brings forth the need to modify the terminology to

be able to quantify a wider class of failures associated with liquefaction. Florin and Ivanov (1961) used the word 'liquefaction' to describe the behavior of a horizontal layer of loose sand when compacted by blasting. If the pores were full of air that could flow out quickly, the layer would quickly settle. If the pores are full of water, that flow takes time. In that brief period, the soil grains are suspended in an upward flow of pore fluid, like an upward seepage flow fluidizing sand in the floor of a coffer dam. Chemical engineers have used fluidized beds, for example, in some heat transfer processes. Thus, a detailed examination of the terms *liquefy* and *fluidize* may enable us to better describe the failures in soils.

Hazen's Liquefaction

Schofield (2005) described Hazen's liquefaction as a phase transition caused by an unstable chain reaction. Discrete soil particles are held together by the high stress they carry. Under a sudden force, one grain will slip and release the elastic stress it carries to the surrounding pore water. Immediately, the other soil grains fall apart "like a house of cards." All the unstressed particles flow in the water, as if the soil had melted. Think of how sharply striking wet sand "makes quicksand for only a few seconds until the surplus water can find its way out." Casagrande expanded on Hazen's liquefaction to explain that contractive soils are prone to liquefaction, while a dilative soil is generally safe. In a dilative soil, the soil structure expands under shearing, and so does not transfer any stress to the pore pressure. Casagrande noted in 1975, however, that even dense sand can liquefy under sufficiently high load.

Herrick's Liquefaction

Herrick's liquefaction was named by Schofield (2005) after a poem written by Robert Herrick, an English country parson, in the 1600's.

Upon Julia's Clothes

Whenas in silks my Julia goes,

Then, then, methinks, how sweetly flows

That liquefaction of her clothes.

Next, when I cast mine eyes and see

That brave vibration each way free;

O how that glittering taketh me!

The above poem captures the idea that in the total absence of stress, a material will liquefy. But as Schofield pointed out, zero stress alone is not a complete criterion for liquefaction. A mechanism is required to put the particles in motion, just as Julia's movements put the silk into temporary motion. He used the example of sand grains resting on the surface of a desert dune or a seabed, which are under zero effective stress. The grains do not move, however, until the wind in the desert or the current in the sea mobilize the soil particles. For Herrick's liquefaction, the soil grains must be near zero effective stress *and* be subject to a hydraulic gradient, causing fluid flow powered by gravity. Without the presence of the hydraulic gradient, the particles will remain interlocked, even though they are under zero stress. When the soil liquefies, there is no unstable release of energy, as with Hazen's liquefaction.

Liquefaction and Fluidization

Notably, Herrick's poem molded the vocabulary used to describe soil behavior. The Concise Oxford English Dictionary defines 'liquefy' as 'make or become liquid,' a liquid being described as 'a substance that flows freely.' It says 'fluidize' means 'to cause a finely divided solid to acquire the characteristics of a fluid by passing a gas upwards through it.' A fluid is defined as 'a substance that has no fixed shape and yields easily to external pressure.' In the Middle Ages, 'liquefaction' was thought by Christians to be the phenomenon of blood flowing from the wounds of a statue of Jesus Christ, and also the melting of a soul. Herrick used the word in a secular sense, thus opening the opportunity for Hazen to adopt the word for his purposes. Herrick had used the word for an unconventional meaning, but Hazen seems to ignore this fact, and brought liquefaction the meaning we attribute to it today. Liquefaction describes unstressed grains flowing into solution of the surrounding pore water. Fluidization is when water flows through soil and carries the particles with it into suspension, as with water filling a trench.

Youd et al (2001) summarized the modern definition of liquefaction as 'the transformation of granular material from a solid to a liquefied state as a consequence of increased pore-water pressure and reduced effective stress.' This results in a significant loss of shear strength in fine-grained soils. Furthermore, in moderately dense soils, 'liquefaction leads to transient softening and increased shear strains,' and cyclic mobility may follow.

This study uses the critical state soil mechanics to define the wider class of failures associated with soil deformation as a function of the combination of void ratio and confining stress in the next chapter. As will be seen, the critical state definition of liquefaction follows closely the definition of Herrick's. More importantly, it is used to develop a criterion for the

liquefaction of fine grained soils. In order to facilitate its development in the context of current research, the current chapter concludes with a review of criteria for fine grained soil liquefaction. Most of these criteria are ad hoc modifications based on some notable observations by Chinese researcher Dr. Wang Wenshao; thus the term Chinese criteria are often used in the literature.

Chinese Criteria

In 1979 Dr Wang Wenshao published his research of major earthquakes in China between 1966 and 1976. Many of these earthquakes showed surface evidence of fine-grained soil liquefaction, particularly the Haicheng and Tangshan earthquakes, in 1975 and 1976, respectively. Wang found that the common characteristics of the liquefied fine-grained soils were having less than 20% clay content (5μm or less), liquid limit between 21 and 35, plasticity index between 4 and 14, and a natural water content above 90% of the liquid limit. The plasticity characteristics of the original Wang (1979) data are shown in Figure 2-2. Seed and Idriss (1982) modified Wang's conclusions, and defined the liquefaction criteria of fine-grained soil to be a clay fraction (5μm or less) less than 15% by weight, liquid limit less than 35, and water content greater than 90% of the liquid limit. Liquefaction will occur *only* if all three criteria are met. These requirements are called the 'Chinese criteria,' after their origins. The Chinese criteria are the current accepted method for evaluating liquefaction potential of fine-grained soils.

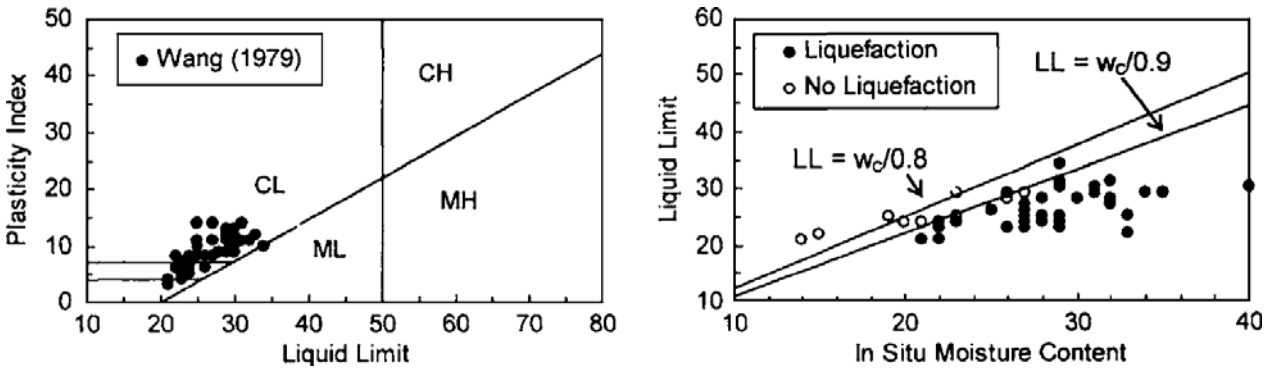

Figure 2-2. Data analyzed by Wang (1979) in the development of the Chinese criteria (Bray and Sancio 2006)

Recent field observations have necessitated the need for re-evaluation of the Chinese criteria. Three recent earthquakes, the 1994 Northridge, 1999 Kocaeli, and 1999 Chi Chi earthquakes, all showed evidence of liquefaction in soils with greater than 15% clay content. This means the soil did not meet all three of the Chinese criteria, and yet still liquefied. Liquefaction of soils in Adapazari, Turkey during the 1999 Kocaeli earthquake led to much of the damage throughout the city, even though they typically had clay contents greater than 15% (Bray and Sancio 2006). After the 1994 Northridge earthquake, Holzer et al (1999) noted that soils that would have been determined safe from liquefaction by the Chinese criteria did in fact liquefy and lead to permanent ground deformations.

Although Youd et al (2001) established the Chinese criteria as the current state-of-the-practice for liquefaction susceptibility of fine-grained soils, many current researchers, such as Bray and Sancio (2006) and Boulanger and Idriss (2006), recommended not relying on the Chinese criteria. The Chinese criteria are based solely on plasticity characteristics, and do not account for the confining stress of in-situ soil. One plasticity criterion is chosen to be applicable. Wang's research shows that soils with water content-liquid limit ratios less than 0.9 did not liquefy, except in one case with a ratio only slightly less than 0.9. Soils with water

content-liquid limit ratios greater than 0.9 all liquefied, again except for one case, in which the ratio was only slightly greater. This criterion appears to be important in evaluating liquefaction susceptibility; however, the other two Chinese criteria may not be valid. Wang's data from 1979 does not show the behavior of any soil with a liquid limit greater than 35, and recent earthquakes have revealed liquefied soils with greater than 15% clay fractions.

Andrews and Martin (2000) concluded that the criteria for liquefaction susceptibility should not include a water content-liquid limit ratio as a condition for silty soils. Additionally, they reduced the liquid limit criterion to LL < 32, and the clay fraction condition to < 10% clay particles. They used 2 μm as the definition of clay-sized particles, which is smaller than the previously used 5 μm. If a soil meets only one of the two criteria, further study is required to confidently evaluate liquefaction susceptibility. Figure 2-3 graphically shows the Andrews and Martin (2000) criteria, in which filled circles represent specimens meeting all conditions of the criteria. Polito (2001) determined three categories of liquefaction susceptibility, based on plasticity characteristics. A soil is liquefiable if LL < 25 and PI < 7; soils with 25 < LL < 35 and 7 < PI < 10 are potentially liquefiable; and 35 < LL < 50 and 10 < PI < 15 indicates a soil susceptible to cyclic mobility. Perlea (2000) recommended lab testing as the best evaluation method for liquefaction potential.

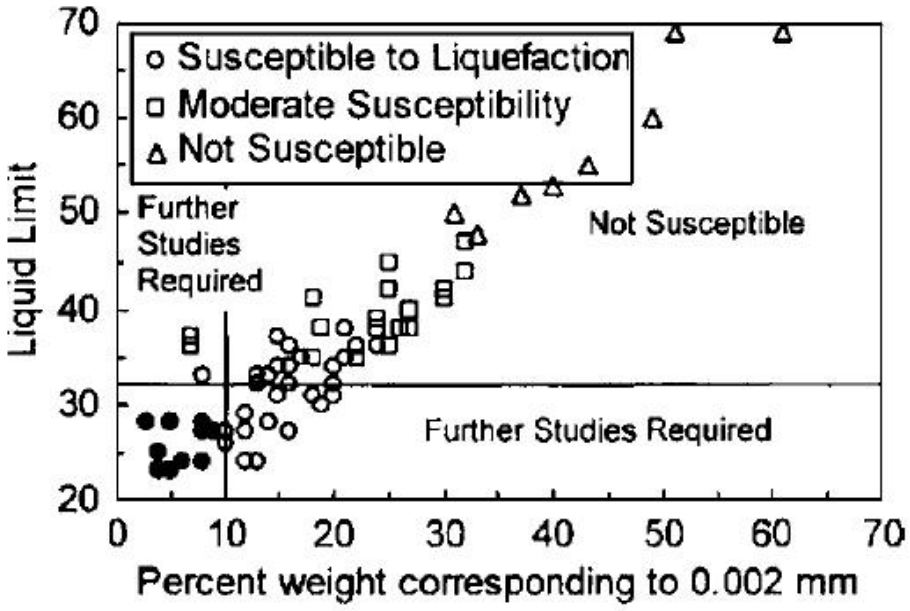

Figure 2-3. Andrews and Martin (2000) criteria for liquefaction (Bray and Sancio 2006)

Boulanger and Idriss (2006) suggested that 'sand-like' fine-grained soils and a 'clay-like' fine-grained soils respond differently to cyclic loads. A sand-like soil is susceptible to liquefaction, while a clay-like soil will respond with a cyclic failure. Plasticity index is used to determine the difference between the two categories. A PI < 7 indicates sand-like liquefaction susceptibility, while soils with a PI ≥ 7 are considered clay-like, prone to cyclic failure.

CHAPTER 3
CRITICAL STATE FRAMEWORK

Critical State Soil Mechanics

The critical state framework recognizes that soil is a frictional material of interlocking particles and that it shows three distinct classes of behavior, which depend inherently on density and effective pressure. As illustrated in Figure 3-1, at great depths, the high confining stress will cause ductile yielding and the soil will fold. A soil under lower pressure will fail by rupturing, and the soil will exhibit faults with gouge material present along the slip planes. Soils at the lowest confining stress, near the surface, will fracture and form fissures.

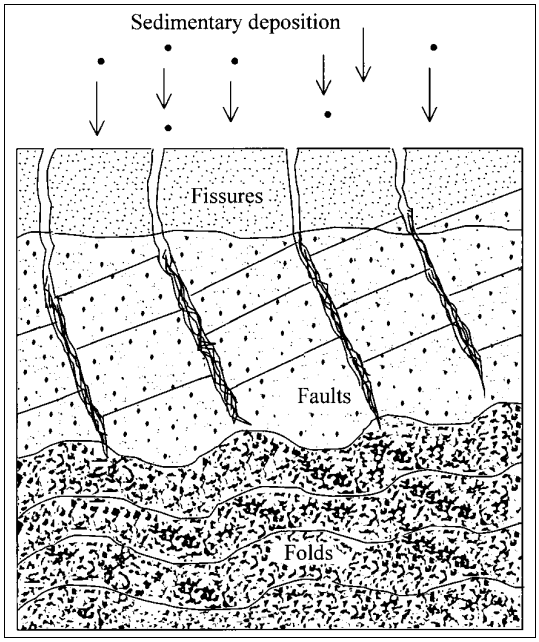

Figure 3-1. Sedimentary deposit behavior (Muhunthan and Schofield 2000)

The critical state framework defines the state of a soil with three variables: p', mean normal effective stress; q, deviatoric shear stress; and ν, specific volume ($\nu = 1+e$, where e is the void ratio). The first two are defined for a triaxial compression test as:

$$p' = (\sigma'_1 + \sigma'_2 + \sigma'_3)/3 = (\sigma'_1 + 2\sigma'_3)/3 \quad (3\text{-}1)$$

$$q = \sigma'_1 - \sigma'_3 \quad (3\text{-}2)$$

where σ'_1 and σ'_3 are principal effective stresses.

Roscoe, Schofield, and Wroth (1958) state that soils attain an ultimate state at which there is no change in mean normal effective stress, shear stress, or specific volume as the soil continues to deform. At this point, the state of the soil lies on a unique critical state line, which lies in the three-dimensional (p', q, ν) space. For simplicity, two-dimensional representations are often used for ease in visualization.

On the (ν, ln p') space, as shown in Figure 3-2, the critical state line is defined by:

$$\Gamma = \nu + \lambda \ln p' \quad (3\text{-}3)$$

where λ is the slope of the line and Γ is the intercept at the ν-axis.

On the same (ν, ln p') space, the elastic compression and swelling of a soil will generally follow a line described by:

$$\nu_\kappa = \nu + \kappa \ln p' \quad (3\text{-}4)$$

where ν_κ is the intercept of the line with the ν axis and κ is the slope of the line.

The elastic compression and swelling characteristics of the aggregate determine the slope, while the packing density of the aggregate particles defines the intercept.

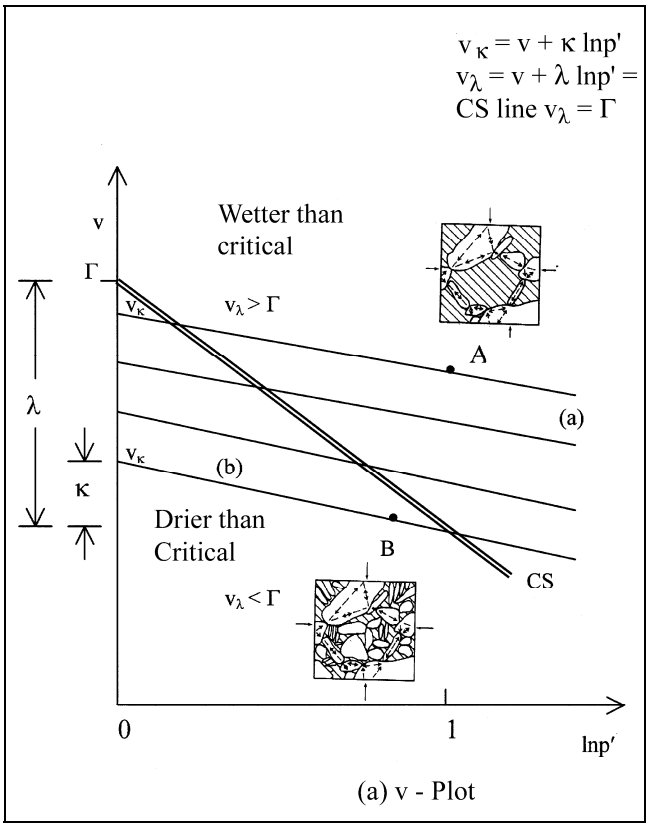

Figure 3-2. Aggregate behavior and critical state (Muhunthan and Schofield 2000)

The influence of packing density on soil behavior is illustrated in the insets of Figure 3-2. The load on a soil is carried at the contact points between individual grains. An aggregate made up of a skeleton of load-bearing particles with very few 'filler,' lightly-stressed particles in the voids of the load-carrying grains will have a higher intercept. This is considered an 'open packing' configuration (see point A of Figure 3-2). As the volume is filled in with lightly-loaded grains, the soil becomes densely packed, which will result in a lower intercept value, as with point B of Figure 3-2. Since the filler particles do not carry load, the soil is at the same stress; therefore the compressibility of the soil remains the same, as indicated by the equal slopes of lines (a) and (b) in Figure 3-2.

Consider these two specimens are subjected to shear, causing plastic deformation, while the pore water is allowed to drain. Under these conditions, the soil with the open packing is contractive. As the supporting skeleton collapses, the soil compresses. Conversely, the densely-packed soil will dilate under shear. Since the voids are filled with the lightly-loaded grains, the particles will slip and ride over each other, resulting in a volume increase. For every aggregate there is a certain packing density for which the collapse and expansion are in balance during shear, and there is no change in volume. This is the point of critical state: sustained shear load at a constant mean normal effective stress and with no volume change, only a rearrangement of the grains.

All aggregates will eventually reach critical state when plastic shear is applied. As the skeleton of loosely-packed specimen collapses, the former load-supporting particles become unstressed and fall into the voids as filler particles. The soil is now more densely packed, and ν_κ drops. A densely-packed specimen dilates, with a rise in ν_κ. Regardless of the initial packing density, the aggregate will tend toward the critical state packing density, as illustrated by the stress paths approaching the critical state line in the (ν, ln p') space. When it reaches critical state, the load carrying structures will continually form and collapse as successive new structures are formed, without a change in the packing density. It is at this point the state of soil will plot on the critical state line, defined in Equation 3-3 (Muhunthan and Schofield 2000).

The 3-D (p', q, ν) space behavior of the soil behavior is represented in a 2-D space by using a number of normalization procedures. The first representation normalizes the data with the critical state pressure, p'_{crit}, as shown in Figure 3-3. The soil behavior represented in this space shows three distinct regions: the fracture, fault, and fold regions. The point of critical state is at point B, where $p' = p'_{crit}$. When stress is less than the critical stress, the soil will rupture, as

shown by line AB, which follows the Mohr-Coulomb failure surface. Under very low stress, a soil will fracture, shown by line OA, which has a slope of 3. When the critical pressure is reached and exceeded, the soil folds in ductile yielding, shown by the Cam clay line BD (Muhunthan and Schofield 2000).

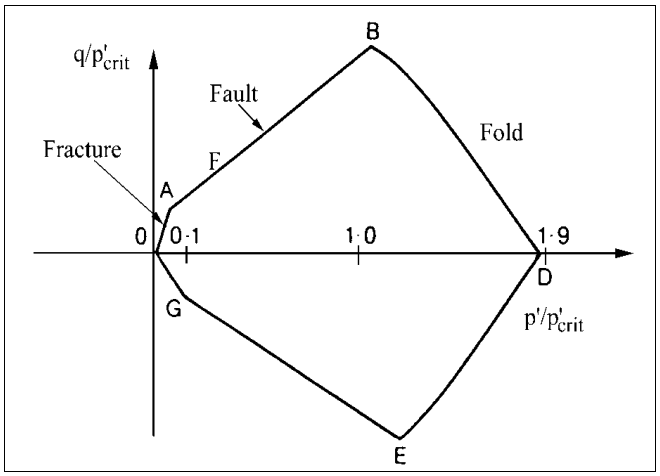

Figure 3-3. Normalized plot of q vs p′ (Muhunthan and Schofield 2000)

The behavior map of the three distinct regions can alternatively be shown in terms of the stress ratio η, which is defined as:

$$\eta = q / p' \tag{3-5}$$

This plot is obtained from the normalized q/p'_{crit} vs p'/ p'_{crit} plot by drawing a fan of straight lines as shown in Figure 3-4. A straight line drawn from the origin of the q vs p′ plot has slope η. The value of p′ wherever such a line crosses the q vs p′ line determines a data point in the (η, p′) space. The resulting regions of failure in (η, p′) space are as shown in Figure 3-5. It can be seen that the fracture region has a constant η = 3, followed by a curvilinear form for the fault region, and a linear segment representing the cam clay yield region.

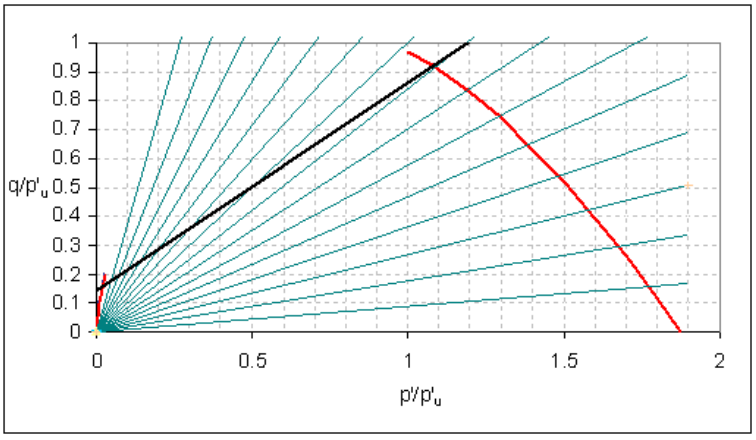

Figure 3-4. Normalized q vs p′ plot with radiating stress ratio η lines

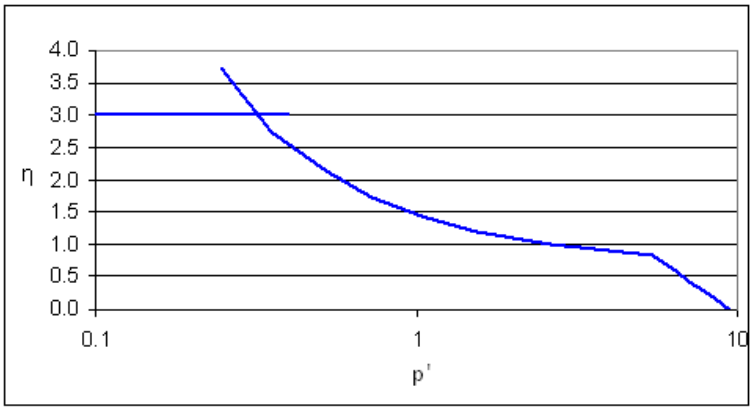

Figure 3-5. Failure surface in (η, p′) space, as derived from the normalized q vs p′ plot

Equivalent Liquidity

The regions of soil behavior identified in the (η, p′) space can be expressed using basic physical properties of soil. These properties include measures such as the liquid limit (LL) and the plastic limit (PL) that define the plasticity characteristics of soils. In particular, the liquidity index, LI defined as:

$$LI = (w - PL) / (LL - PL) \quad (3\text{-}6)$$

where w = in-situ water content becomes a useful parameter for converting the mean stress values as shown below.

According to Schofield (1980), the critical pressure of a soil at the liquid limit is 5 kPa, and p'_{crit} at the plastic limit is 500 kPa. These values are two log cycles apart, so the horizontal axis of Figure 3-6 can be shown on a log p′ scale. Assuming the lower limit of yield occurs at $p/p'_{crit} = 1.0$ (see Figure 3-3), the LI will be 1.0 at the plastic limit, when p′ = 5 kPa. This means the line separating the fracture zone from the rupture zone, also known as the critical state line, will intersect the vertical, LI axis at 0.5 and the horizontal, log p′ axis at 50 kPa. Similarly, the line separating the fracture and rupture zones intersects LI = 0.5 and p′ = 50 kPa, and parallels the critical state line.

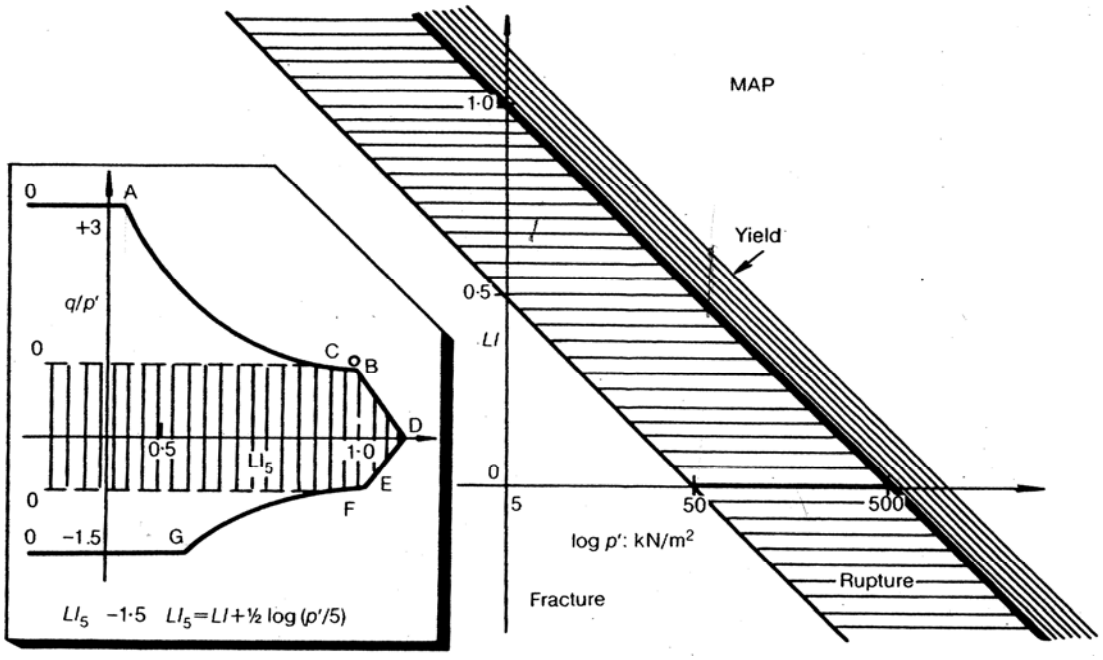

Figure 3-6. Liquidity and limits of soil behavior (Schofield 1980)

States of soil may plot at any point on the graph in Figure 3-6. To more easily determine in which behavior region a state of soil will lie, the equivalent liquidity LI_5 is found by projecting

the state of soil to the $p' = 5$ kPa axis in the direction parallel to the critical state line. The equivalent liquidity can also be found numerically using the definition of LI_5:

$$LI_5 = LI + 0.5 \log (p' / 5) \tag{3-7}$$

where p' is in units of kPa.

The equivalent liquidity, then, describes the liquidity of the soil with an adjustment for the in-situ pressure. As can be seen in Figure 3-6, an LI_5 value of less than 0.5 indicates the fracture zone. A value between 0.5 and 1.0 would plot in the rupture zone, while a value greater than 1.0 represents the ductile failure zone.

The inset of Figure 3-6, a plot of LI_5 versus the stress ratio η, shows the failure surface when p' is constant. In general, the stress ratio increases as the equivalent liquidity drops, but the change is not continuous. The three regions of behavior clearly appear in this stress-liquidity space. When LI_5 is near zero, the soil is in the cracking zone. This horizontal line OA on the compression side is at $\eta = 3$ because $\sigma'_3 = 0$ when pressure, or equivalently, LI_5, is near zero. Similarly, in tension, $\sigma'_1 = 0$ in the near-zero condition, so $\eta = -1.5$, shown in line OG. The curved lines AC (in compression) and GE (in tension) indicate the region of rupture. Critical state is reached at the highest value of LI_5 in this zone. The area to the left of critical state on the plot is considered the 'dry' side, while to the right of critical state is called the 'wet' side. The failure mechanism on the wet side of critical state is ductile yielding, where the increase in stress ratio is linear, as shown in lines CD and ED. When the effective stress path of a specimen reaches the failure surface, it will fail under the respective limiting behavior. States of stress that plot outside of the surface are considered unstable.

Liquefaction in the Critical State Framework

Liquefaction susceptibility of a soil depends on the plasticity characteristics of the soil as well as the effective in-situ stress and the applied earthquake load. Therefore, the LI_5 space is ideal for representing states of stress when discussing liquefaction susceptibility. In general, a state of stress with $\eta < 1.0$ and within the yield surface, shown in the shaded region of the inset of Figure 3-6, is stable. This is where the deviator stress is equal to or less than the average normal stress. States of stress above $\eta = 1$ and within the fracture zone ($LI_5 \leq 0.4$), or outside of the cam clay region, are unstable and likely to liquefy under cyclic loading.

The cyclic loading of an earthquake causes an increase in the deviator stress q, which therefore causes a change in the shear stress. An increase in q could shift the state of stress outside of the safe zone, particularly if the stable state of stress is near the boundary. The average shear stress caused by an earthquake load can be determined by the critical stress ratio, CSR, shown in Equation 3-8.

$$CSR = \tau / \sigma'_v = 0.65 \, (a_{max} / g) \, (\sigma_v / \sigma'_v) \, r_d \qquad (3\text{-}8)$$

where τ = average shear stress

σ'_v = effective vertical stress

σ_v = total vertical stress

a_{max} = maximum ground acceleration

g = acceleration due to gravity

r_d = depth reduction factor.

For this study, the depth reduction factor recommended by Rauch (1997) is used. This factor can be written as:

$$r_d = 1.0 + 1.6E\text{-}6 \, (z^4 - 42z^3 + 105z^2 - 4200z) \qquad (3\text{-}9)$$

where z is the depth below the ground surface in meters. This equation is valid to 30 meters. All data used for this study is at a depth of 30 meters or fewer.

Since $q = \sigma'_1 - \sigma'_3$ (Equation 3-2) and $\tau = (\sigma'_1 + \sigma'_3) / 2$, the additional deviator stress on a sample caused by the applied shear stress of a cyclic load is twice the average shear stress, as shown in Equation 3-10.

$$\Delta q = 2 \tau \tag{3-10}$$

When Δq is added to the initial q, a state of stress will shift vertically upward in (η, p') space. Pore water pressure also increases, reducing p', and the state of stress will also shift slightly to the left. If a soil shifts above the $\eta = 1$ line while in the fracture zone ($LI5 \leq 0.4$), or outside of the cam clay region, it is likely to liquefy. For earthquakes with higher ground accelerations, the added deviator stress will be higher when all other variables are equal, resulting in a larger shift. Soils subjected to stronger earthquakes consequently could have a higher susceptibility to liquefaction. Different vertical effective stresses have a minimal effect on the shift in deviatoric stress because as normal stress increases, the depth reduction factor decreases, and the opposing changes have a general balancing effect.

Recall that the apparently valid Chinese criterion for liquefaction is that water content be greater than or equal to 90% of the liquid limit. When $w = 0.9LL$, LI is very close to 1 (refer to Equation 3-6), where the soil reaches critical state failure. Hence, this criterion generally works.

CHAPTER 4
DATA ANALYSIS

General

This chapter presents an analysis of observed field data relating to studies of the liquefaction of fine-grained soils based on the critical state framework. Comparisons to those made by the Chinese criteria are made wherever possible. The critical state framework enables the effect of two significant parameters (peak ground acceleration a_{max}, and depth) on liquefaction potential to be analyzed systematically. Finally, the importance of cementation bonding on liquefaction of sensitive clays is considered.

Field Data

Data used in this study consists of those used in Wang's study (1979) and Standard Penetration Test (SPT) borings of post-earthquake liquefied sites in Turkey and Taiwan. Wang's data was for soils that liquefied in the Haicheng and Tangshan earthquakes, in 1975 and 1976, respectively. The SPT boring sites all included fine-grained soils. SPT data from six liquefied 1999 Kocaeli earthquake sites were downloaded from the website http://peer.berkeley.edu/publications/turkey/adapazari/ index.html. SPT boring logs from 35 sites that liquefied during the 1999 Chi-Chi earthquake were downloaded from the websites http://peer.berkeley.edu/lifelines/research_projects/3A02/ and http://www.ces.clemson.edu/chichi/TW-LIQ/In-situ-Test.htm (Papathanassiou 2008). The moment magnitude M_w of the Kocaeli earthquake was 7.4 and of the Chi-Chi earthquake was 7.6. The SPT data for the Kocaeli earthquake sites are from the towns of Adapazari and Yalova, where the maximum ground accelerations (a_{max}) were both recorded as 0.4g (Papathanassiou

2008). The borings for the Chi-Chi earthquake were performed in the towns of Yuanlin, Nantou, Wufeng, and Dachun, where the average PGA values were 0.18g, 0.38g, 0.67g, and 0.19g, respectively (Papathanassiou 2008).

Critical State Failure Surface

In order to examine the data from the critical state framework, functional forms of the various segments of the critical state failure surface in the (η, LI_5) space (Figure 4-1a) needed to be determined. In the absence of laboratory data, it was decided to obtain this from the normalized (q, p′) plot for Weald clay presented by Schofield and Wroth (1968). Data from other soils (Schofield 1980; Lawrence 1980) show that the overall shape and the regions of the state surface remain the same while the transition numbers may change slightly. To derive this failure surface, straight lines radiating from the origin, as shown in Figure 4-1b, were extended in five-degree increments to the lines showing the regions of folding, faulting, and fracturing. The radiating lines have angle α, and the tangent of α is the value η. Corresponding LI_5 values for each α line are found using the value of p' / p'_u at the intersections of the radiating α lines with the plot.

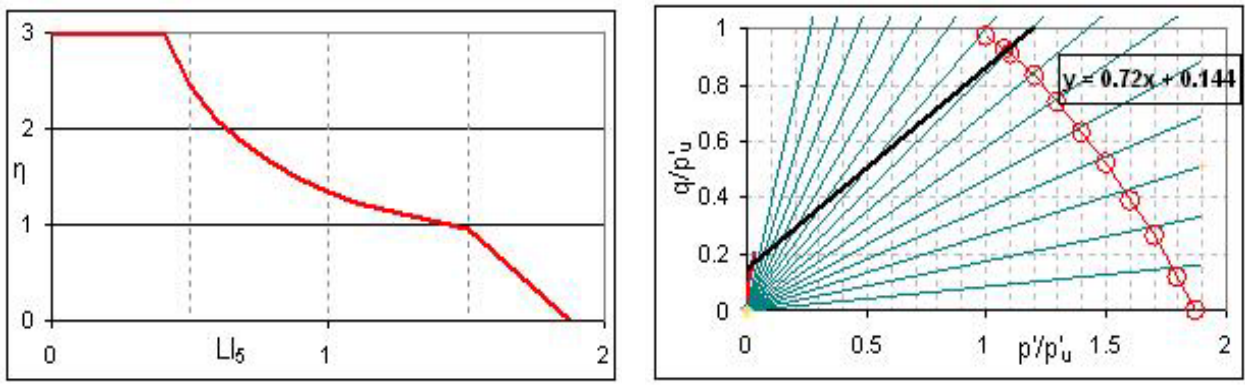

(a) (b)

Figure 4-1. Critical state failure surface and its derivation

The best fit lines of the different segments of the surface, shown in Figure 4-1a are as follows:

Fracture	$\eta = 3$	when $0 < LI_5 < 0.4$	(4-1a)
Fault	$\eta = 1.35\ (LI_5)^{-0.87}$	when $0.4 < LI_5 < 1.5$	(4-1b)
Fold/yield	$\eta = -2.53\ (LI_5) + 4.75$	when $1.5 < LI_5 < 1.875$	(4-1c)

The above equations are used in determining the type of soil behavior expected in the field. Soils become susceptible to liquefaction ("unsafe") when they shift above the $\eta = 1$ line in the fracture zone ($LI_5 \leq 0.4$), or if they plot outside of the cam clay region. Soils that lie outside of the cam clay region remain stable due to interparticle bonding, which can be broken under earthquake loads. The effect of bonding is discussed at the end of this chapter.

At-Rest Data on the Critical State Diagram

From the SPT soil data and the Wang (1979) soil data, the liquidity index and the mean effective confining stress were determined. These values were used to determine the equivalent

LI_5 values. The vertical effective stress was determined at the different depths and used to calculate the horizontal effective stress at rest. These values were in turn used to calculate the shear stress ratio η and the LI_5 and η values plotted on the stability diagram to determine the nature of stability of the soils.

The data used in this study for at rest conditions is shown in Figure 4-2. Figure 4-2a shows the field study data from the 1999 Kocaeli earthquake and the 1999 Chi-Chi earthquake on the (η, LI_5) plot. The data used to develop the Chinese criteria were also compared to the (η, LI_5) plot in Figure 4-2b. Most of these soils with $LI_5 > 0$ are stable at rest because they all plot below the η = 1 line. On the other hand, some of the data (circled in red) from Taiwan and Turkey (Figure 4-2a) plot on the negative side of LI_5 axis. These soils are prone to fracture and would result in unstable failures when disturbed by earthquake or other causes. The data points outside the cam clay region boundary may remain stable due to natural bonding (Schofield 1980). They could also be prone to collapse and unstable failure under disturbance. Green data points in Figure 4-2b refer to soils that Wang (1979) identified as nonliquefied.

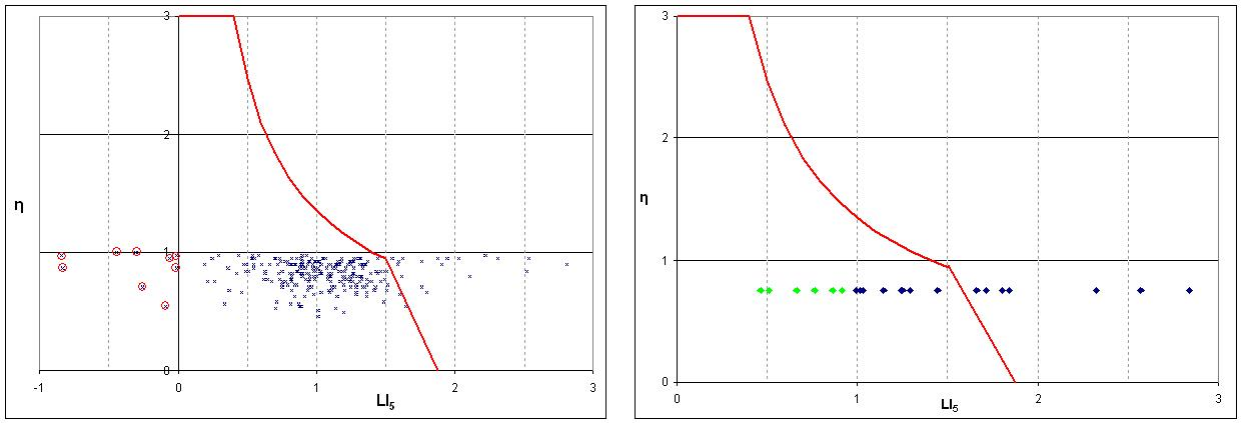

(a) (b)

Figure 4-2. Field study data of in-situ soils at rest

Earthquake Effects on Soil Behavior

During an earthquake, soils undergo shear stresses as well as a rise in pore pressure. Therefore, both q and the effective stress p′ change, resulting in a shift of the shear stress ratio η and equivalent liquidity LI_5. This needs to be determined before further analysis can be made. The value of the deviatory stress Δq is determined from average effective shear stress, τ_{avg}, using the critical stress ratio (CSR). This derivation of Equation 3-10 is described in Chapter 3. Following this process, one can see that Δq is dependent on both the peak ground acceleration of an earthquake and the depth of the soil in question.

Rise in Pore Water Pressure

During cyclic loading the pore water pressure rises. To find p′ during the rise in pore water pressure, first the equivalent number of cycles for the earthquake is determined from the magnitude using Figure 4-3. Then the pore water pressure ratio r_u is found from Figure 4-4 using the equivalent number of cycles and the CSR. The pore water pressure ratio is the ratio of the change in pore water pressure during the earthquake to the effective normal stress,

$$r_u = \Delta u / \sigma' \qquad (4\text{-}2)$$

where r_u is the pore water pressure ratio, Δu is the pore pressure rise, and σ′ is effective normal stress. Thus, the rise in pore water pressure for a given earthquake can be calculated using Equation 4-2. The rise in pore water pressure is subtracted from the existing p′ value to find p′ during the earthquake, which is then used to calculate the stress ratio η. Since rise in pore water pressure decreases the mean normal effective pressure p′, the stress ratio η is increased beyond the shift already caused by depth and a_{max}, as discussed below.

The rise in pore water pressure causes a reduction in the mean normal effective stress p′, an increase in the stress ratio η, and a decrease in equivalent liquidity LI_5. The change in shear stress and pore pressure shifts the state of stress. Oftentimes, such as in an earthquake with a_{max} = 0.5g as seen with the Wang (1979) data in Figure 4-5, the increased shear stress and pore water pressure cause most soils to become unstable, including some of those soils Wang noted as nonliquefied.

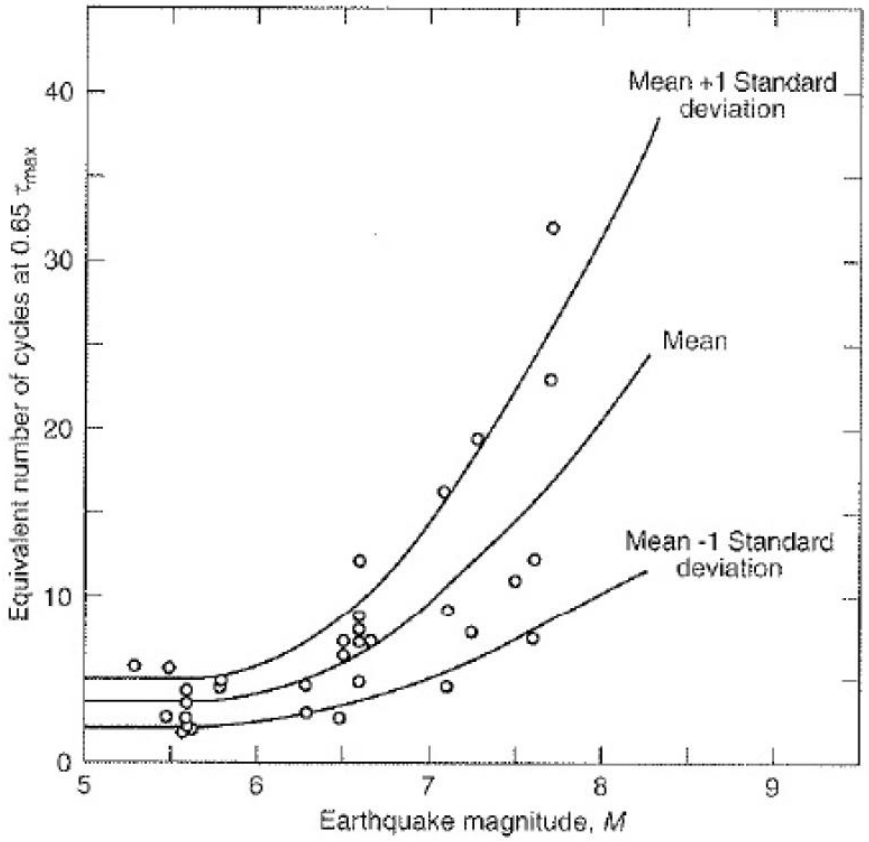

Figure 4-3. Number of equivalent uniform cycles N_{eq} for earthquakes of different magnitude (Kramer 1996)

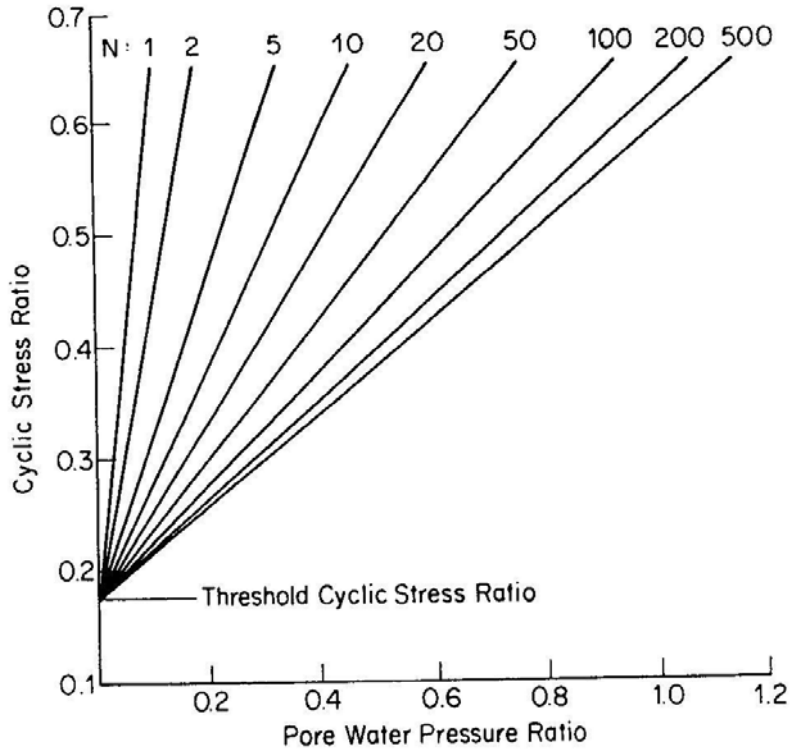

Figure 4-4. Cyclic stress ratio-pore pressure relationship for different numbers of cycles (Ansal and Erken 1989)

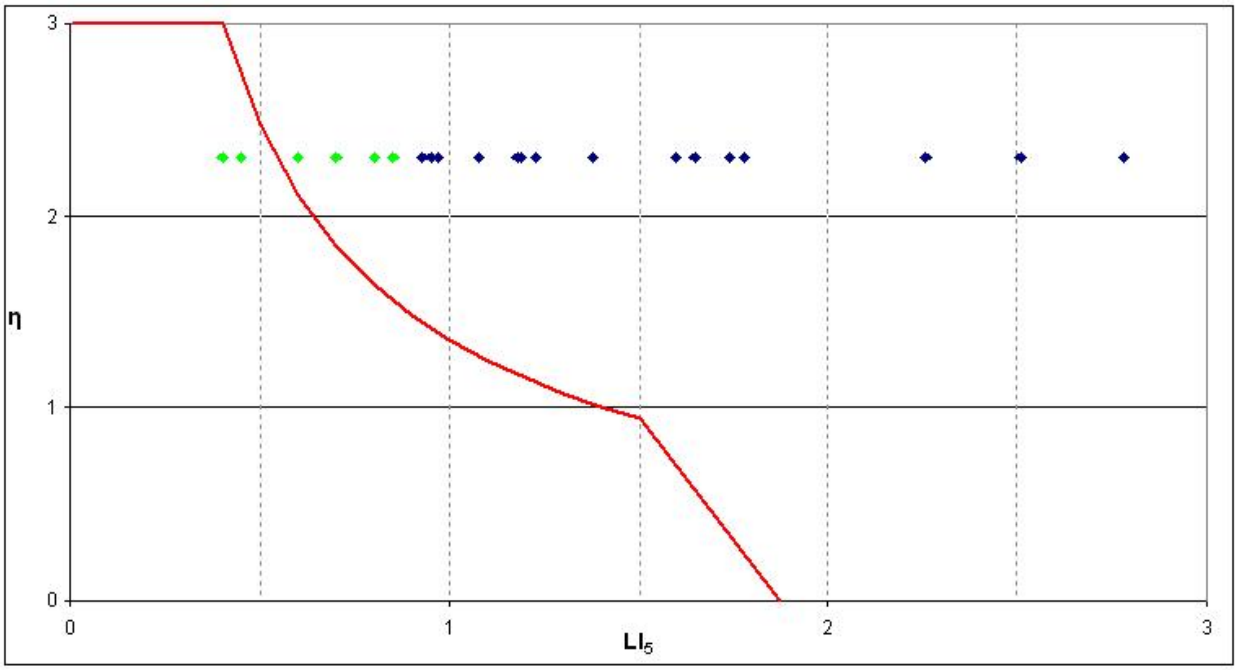

Figure 4-5. Wang (1979) data at 1 meter below ground surface with applied a_{max} = 0.5g

Evaluation of Chinese Criteria Based on Critical State Framework

The SPT data was collected from borings at sites that showed fine-grained liquefaction during an earthquake. Here, only the fine-grained soil layers have been considered. First, each soil was subjected to two of the Chinese criteria: LL < 35 and w ≥ 0.9LL. In the absence of clay fraction data, the clay fraction < 15% criterion was conservatively assumed to be met. The Chinese criteria predicted liquefaction in 13.2% of the soils in the data set. Then, the same data set was evaluated for liquefaction potential using the critical state framework at a range of peak ground accelerations. Data points are plotted on the critical state failure surface plot at various applied earthquake loads, which manifest as shifts in η and LI_5. Under a given a_{max} value, if the point lies above $\eta = 1$ while in the fracture zone, or outside the failure surface, it is considered liquefiable. At $a_{max} = 0.05g$, liquefaction potential was detected in 18.7% of the soils. When $a_{max} = 0.1g$, 34.2% of the soils are identified as liquefiable; when $a_{max} = 0.2g$, the percentage becomes 68.9%; and when $a_{max} = 0.5g$, 99.6% of the data is shown to be liquefiable. When the soils are considered at rest, none are liquefied.

This comparison of assessment methods on known liquefied sites shows that the Chinese criteria are inadequate. Use of the critical state framework would lead to better and conservative estimates because it includes both plasticity and in-situ stress in its parameters, LI_5 and η. It is also more versatile with the incorporation of earthquake load through the parameter a_{max}. The evaluator can determine a maximum a_{max} for acceptable risk in a design situation, or use the maximum likely a_{max} for a site in an analysis of in-situ soils. This approach encompasses a broader number of variables affecting liquefaction susceptibility. It evaluates whether a soil with given plasticity characteristics will liquefy at its in-situ depth under a certain earthquake load, while the Chinese criteria only consider the plasticity characteristics, excluding key information.

Effect of a_{max} on Δq Shift

The size of the shift in shear stress varies according to the applied a_{max}. A very low a_{max} such as 0.05g has a lower effect on the soil. Soils are nudged just over into the unsafe zone of potential liquefaction, as demonstrated by the field study data in Figure 4-6a. Increasingly stronger earthquakes with higher accelerations, however, cause larger shear stress shifts. The shift of a_{max} = 0.15g in Figure 4-6b results in many more unstable states, and an earthquake with a_{max} = 0.5g causes failure in all of the data points, as illustrated in Figure 4-6c.

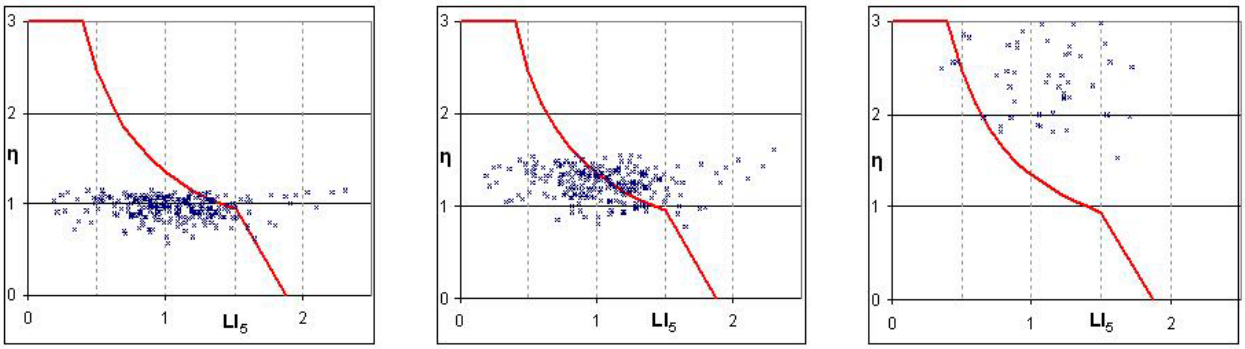

(a) a_{max} = 0.05g (b) a_{max} = 0.15g (c) a_{max} = 0.5g

Figure 4-6. Field study data showing the effect of a_{max} on stress ratio shift

Effect of Depth on Δq Shift

The depth of the in-situ soil also affects the shift in shear stress through the parameters r_d and σ_v. As shown by the data from Wang in Figure 4-7a, an earthquake with a_{max} = 0.5g causes liquefaction for most soils at 1 meter below the ground surface. The same soil found at 20 meters is still safe, as seen in Figure 4-7b.

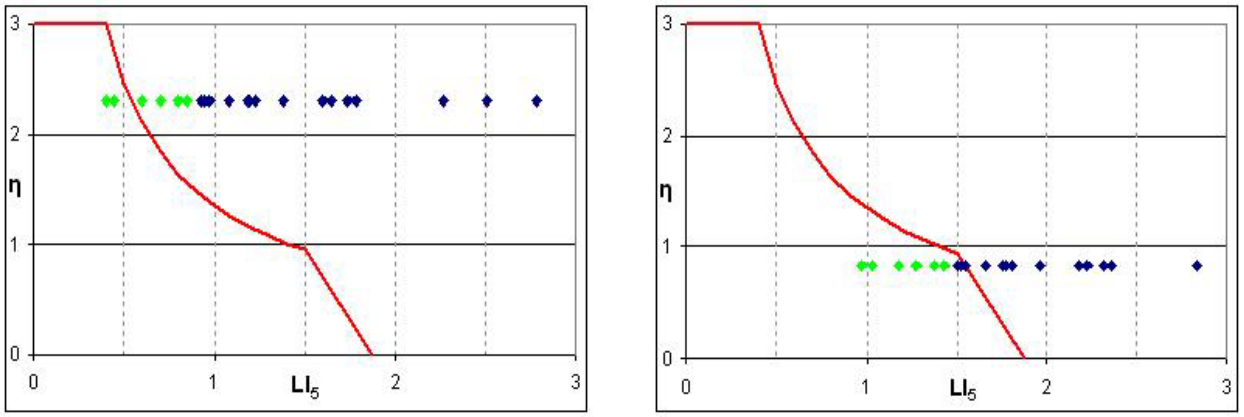

(a) z = 1 meter (b) z = 20 meters

Figure 4-7. Wang data showing the effect of depth on Δq shift within critical state at a_{max} = 0.5g

When all other variables are held constant, it is easily observed that the depth of a soil affects Δq on the same order of magnitude for every a_{max} value. As shown in Figure 4-8, Δq increases with depth until about 9 meters below the ground surface, and then decreases with depth, with the relationship tapering at about 25 meters. Until about 15 meters below the surface, however, the variation is small, adding minimal liquefaction resistance to the soil. Below 15 meters, Δq decreases relatively rapidly. When the shift in deviatory stress is smaller, the jump in η likewise becomes smaller and a soil is less likely to shift into the liquefaction zone. This indicates that 15 meters below the ground surface is a stability threshold when the depth parameter is considered.

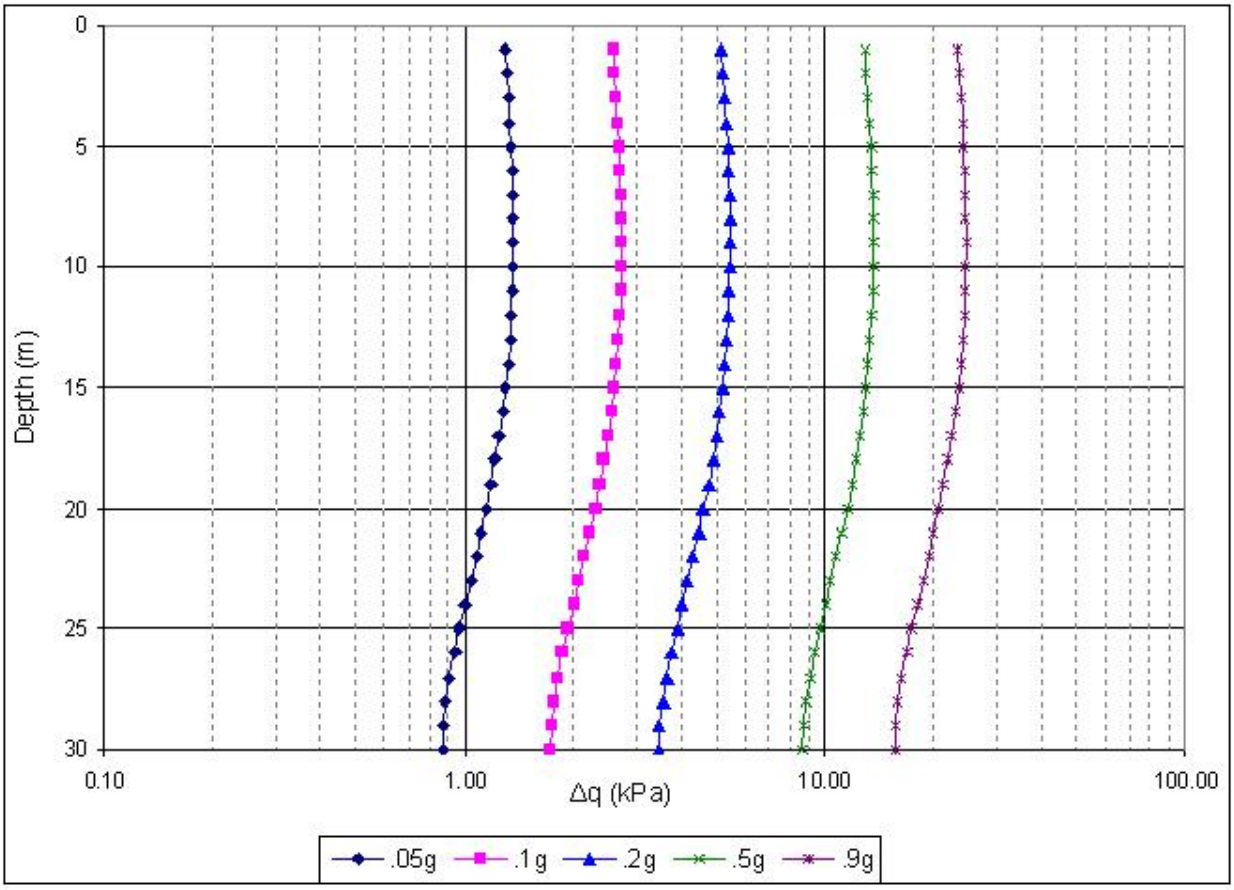

Figure 4-8. Effect of depth on Δq

Shift in Stress Ratio η

The stress ratio η, which is plotted on the vertical axis of the behavior map, is the main factor in determining the safety against liquefaction of a soil with a given LI_5. When $\eta \leq 1$, the soil behavior is stable. The change in deviator shear stress Δq, as well as the rise in pore water pressure, determines the shift in the stress ratio. The effect of the pore pressure rise on the stress ratio is described above. Figure 4-9 shows the shifts in η for a range of LI_5 and a_{max} values. As depth increases, so does LI_5, and as seen in Figure 4-9, when LI_5 is larger the shift in η is smaller. A smaller shift in η makes a soil in the fracture zone less likely to jump into the unsafe zone above η = 1, thereby making it more likely to remain safe. This shows that the same

potentially liquefiable soil becomes safer with depth. The η shift, of course, also depends on a_{max}, so the effect for stronger earthquakes is magnified. For example, if initial LI_5 = 0.4, an earthquake with a_{max} = 0.5g will cause an unsafe jump in η, while the shift for a_{max} = 0.1g remains safe.

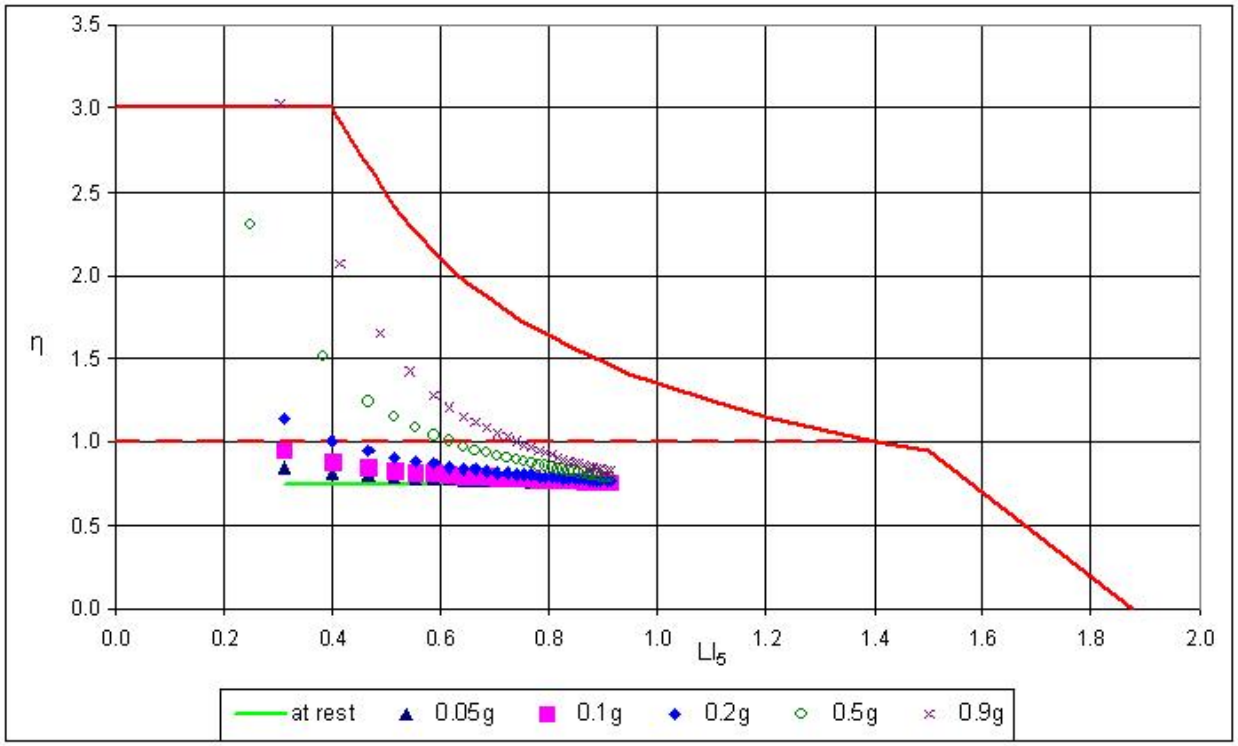

Figure 4-9. Effect of LI_5 on shift in η

The relationship between depth and the shift in η is shown in Figure 4-10. Between 0 and 15 meters below the ground surface, the shift in η under an applied stress is significant, especially at the shallowest depths. Below about 15 meters, the change is much smaller; negligible, even, for the smaller a_{max} values. The data also shows that for an extreme earthquake such as a_{max} = 0.9g, η = 1 when the depth is 13 meters. This indicates, as with the Δq shift with depth, that approximately 15 meters is the reasonable threshold for liquefaction safety, regardless

of the seismic event severity. The stress ratio will not shift to a value greater than 1 under any earthquake force that has been known to occur.

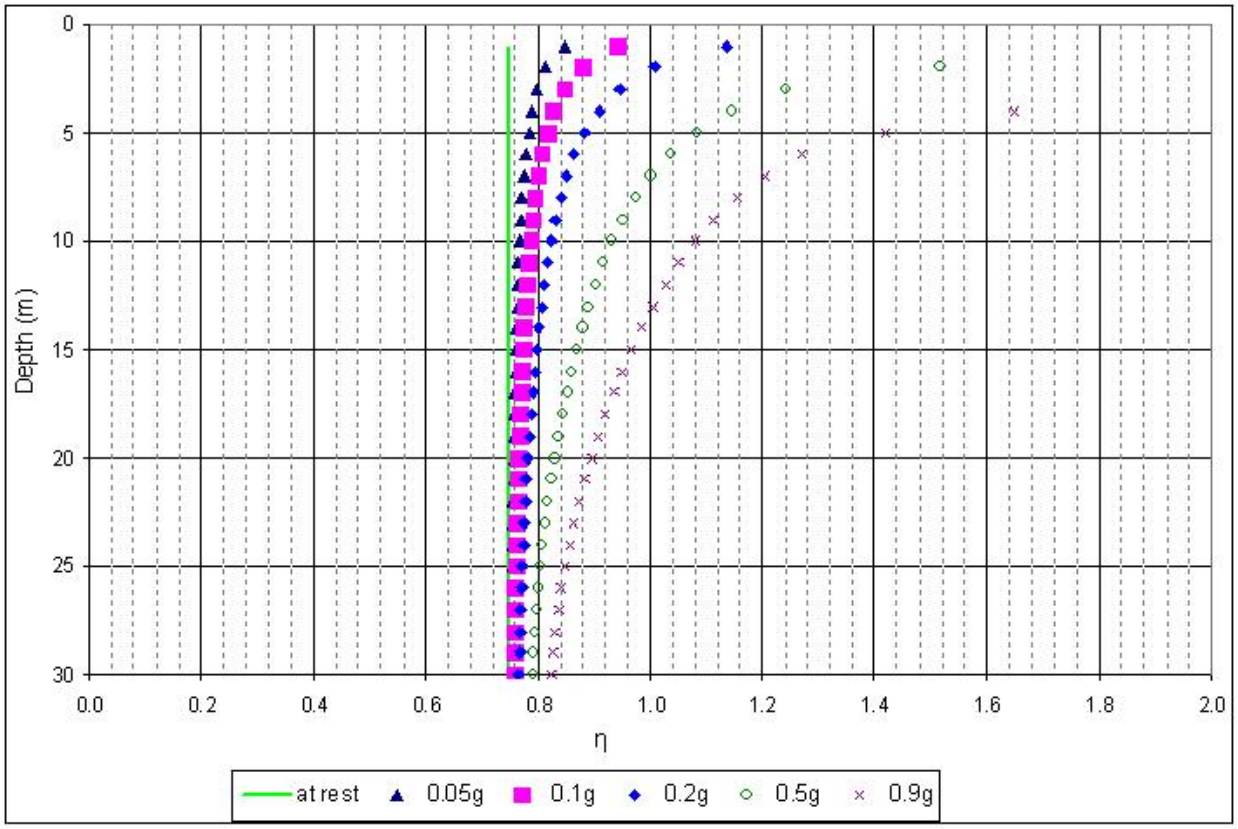

Figure 4-10. Effect of depth z on shift in stress ratio η

Additionally, Muhunthan and Pillai (2009) note in a response to discussion of their 2008 paper on the Teton Dam failure (Muhunthan and Pillai 2008) that a soil's plasticity affects its resistance to large shifts in the stress ratio. For a soil with a PI of about 4, reducing its water content by 2% would reduce its equivalent liquidity index by 50% and the corresponding confining stress by 90%, leading to a big jump in the q/p′ ratio. The same 2% water content reduction in clay with a PI of 20, however, results in an LI_5 reduction by only 10% and a corresponding minor decrease in p′ and increase in q/p′ ratio. This shows that both a soil's depth

and its plasticity characteristics affect how easily η and LI_5 shift into the cracking zone, making the soil susceptible to liquefaction.

Natural Cementation and Bonding

The data points that lie to the right of the failure surface even at rest remain stable due to natural cementation bonding. Sangrey (1972) studied the yield behavior of naturally cemented soils. Cementation can occur in many fine-grained soils from a variety of causes but the unique behavior is similar in all naturally cemented soils. Bonding between particles occurs in-situ, shortly after deposition, from precipitates in water such as calcium carbonate, aluminum and iron hydroxide, or even organic compounds.

Cementation stabilizes a clay when it is at rest because it increases its strength and resistance to deformation at low stresses (Sangrey 1972). The e vs log p curve from compression tests for bonded soils vary from those of uncemented soils by showing a 'lump' in the normal shape, as shown in Figure 4-11. The curve is relatively flat at low stress, and it extends beyond the soil's geologic preconsolidation pressure. The curve then drops abruptly when the cementation bonds are broken and the structure collapses. This occurs at pressure p_c, which is higher than any past stress history of the soil. After the sudden drop, the behavior rejoins the expected curve of the uncemented soil. This 'lump' shows the increased strength due to cementation, but also indicates the soil's danger.

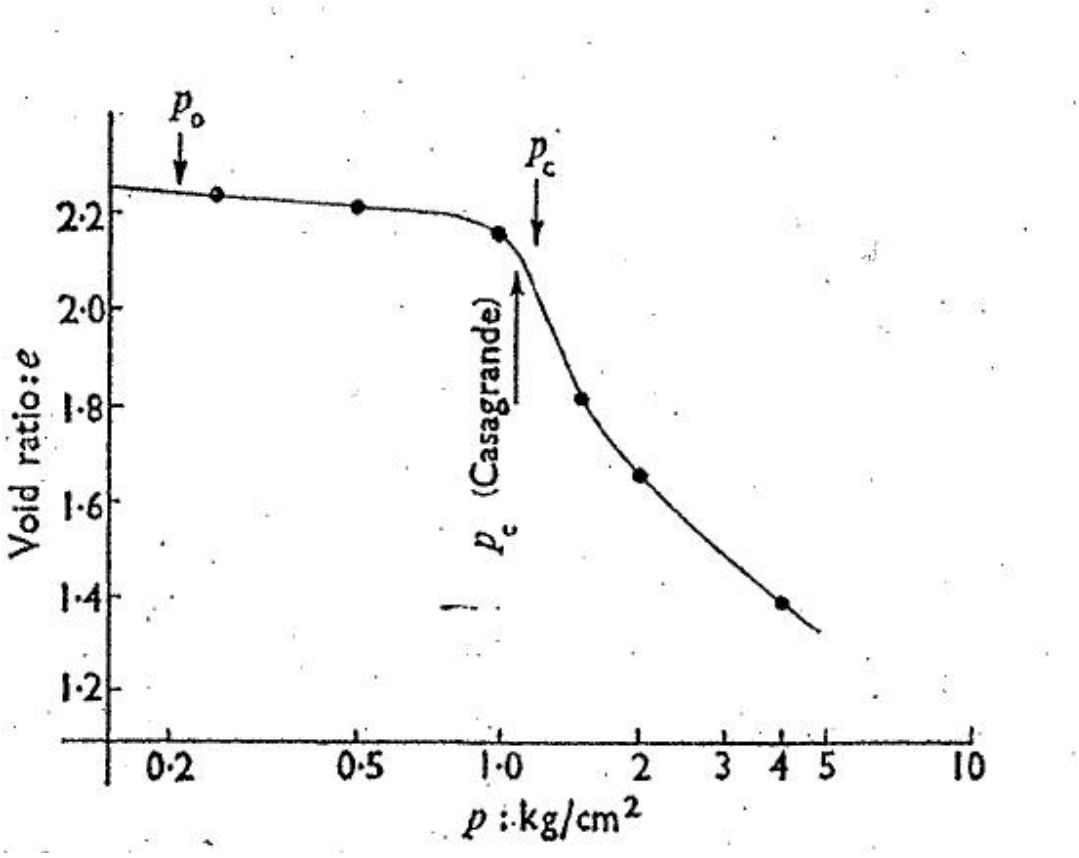

Figure 4-11. Consolidation curve of naturally cemented soil (Sangrey 1972)

For the Labrador clay of Sangrey's study, stability at low stress is illustrated by its failure surface. At low stresses, up to about p′ = 2 kg/cm^2 = 200 kPa, the strength of the cemented soil is higher than typical soils that fail when the effective confining pressure reaches zero. Such soils are highly susceptible to liquefaction throughout a large range of plasticity. In an earthquake, they are very likely to suddenly fail, transferring the confining stress to the pore water pressure. Sangrey's research shows that although cementation increases resistance to deformation, the allowable strain before failure is small, usually less than 1%. Sariosseiri and Muhunthan's (2008) studies on artificial cementation indicate a soil's allowable strain is greatly reduced by cementation bonding. Upon breakdown of the interparticle bonds, both the

magnitude and rate of deformation are large, especially in cases when the pore water pressure increases (Sangrey 1972). In Sariosseiri and Muhunthan's research, all samples exhibited brittle behavior, and the sample with the highest level of cementation failed with a rapid rise in pore water pressure equaling the confining stress and resulting in near-zero effective stress, defining classic liquefaction.

Confining stress, p, affects the failure behavior of cemented clays. In two of Sangrey's tests, he compared the stress-strain curves of the same soil at different confining stresses. As shown in Figure 4-12, both exhibited initial yield, indicating the breakdown of cementation, at the same low strain value. The sample at the lower confining stress then exhibited brittle behavior and quickly lost shear resistance. Sangrey notes, "At low stresses the cementation dominates and little frictional resistance is left once the bonding is destroyed by shear failure. If the rupture is associated with an increase in pore water pressure the frictional resistance is even lower." The sample tested at twice the confining stress of the first, however, displayed a short period of straining at constant shear, and then hardened to a second peak at large strains. This specimen was able to sustain a load and continue yielding after the breakdown of cementation bonds because at a higher confining pressure, it could develop frictional resistance. Lower stresses do not provide sufficient friction. These tests indicate that soils under low confining stresses, e.g. at shallow in-situ depths are more susceptible to sudden unstable behavior. Therefore, liquefaction potential of cemented soils generally decreases with depth, as with uncemented soils.

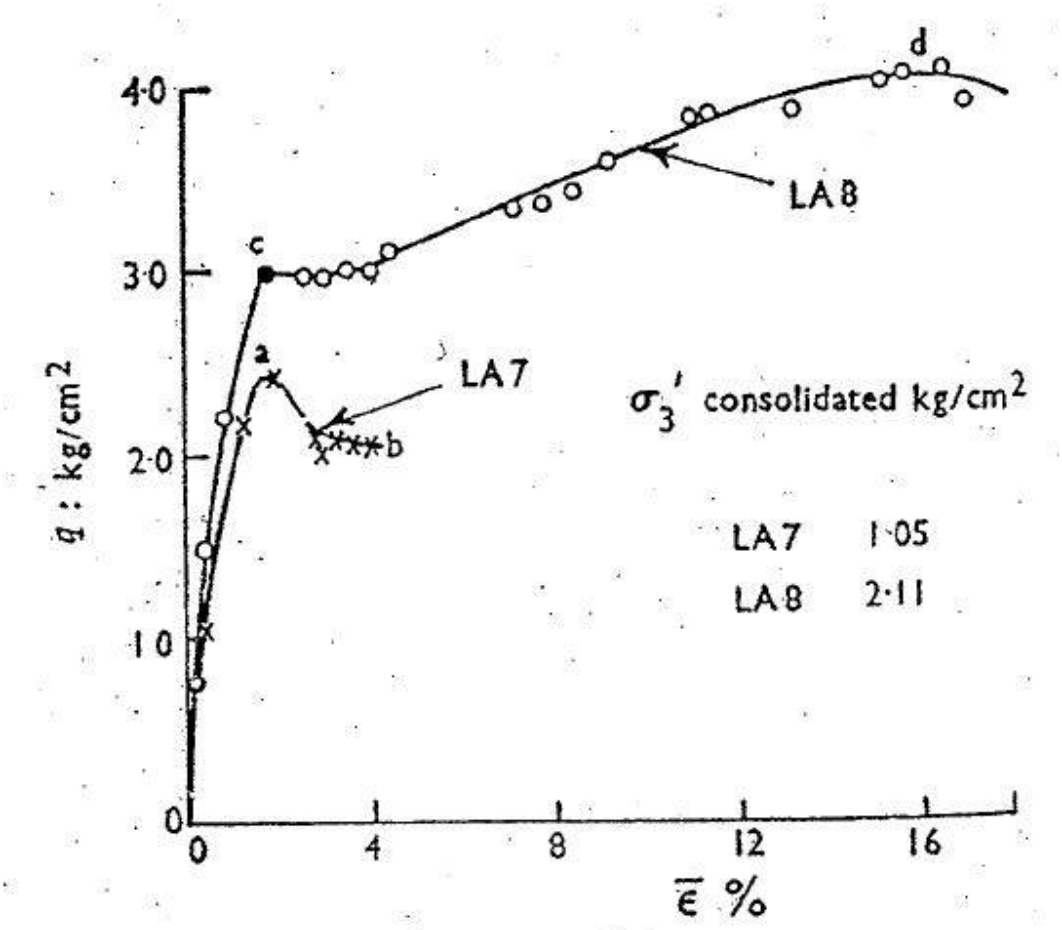

Figure 4-12. Stress-strain curves of naturally cemented soils (Sangrey 1972)

The curves for soil under undrained loads when confining stress is less than p_c, an occasion which would occur in the field in the case of an earthquake, are all similar to the brittle failure of the specimen under low stress (Sangrey 1972). Sangrey mentions that even in the case of high confining stress, under rapid strain (e. g. an earthquake load) there could be moments of undrained behavior in an otherwise drained environment, leading to sensitive behavior of a clay.

CHAPTER 5
CONCLUSIONS AND RECOMMENDATIONS

Conclusions

This study was on the characterization of the liquefaction potential of fine-grained soils. Their liquefaction potential is currently evaluated by the 'Chinese criteria,' based on their plasticity characteristics, introduced by Wang in 1979 based on the study of major earthquakes in China. They were expanded by Seed and Idriss in 1982 and became the commonly accepted method for predicting fine-grained liquefaction susceptibility. More recent research by Boulanger and Idriss (2006) and Bray and Sancio (2006) have shown that the Chinese criteria are ineffective and should not be relied upon to safely predict liquefaction potential. They have proposed modifications to the Chinese criteria for predicting the liquefaction potential of fine-grained soils. None of these criteria, however, account for the confining pressure of in-situ soil or the strength of the earthquake.

It is now known that the shear strength and deformation behavior of soil is very sensitive to the combination of changes in volume and the confining stress. Depending on their combination, a soil aggregate may fracture and crack into clastic debris, or fail with fault planes on which gouge material dilates and softens, or it can continue to yield and deform plastically. The current liquefaction models could not distinguish between these distinct classes of soil behavior and have led to many of the difficulties facing researchers with in the interpretation of liquefaction failures.

This study makes use of the critical state soil mechanics framework, developed in the 1960's, which explicitly recognizes that soil is an aggregate of interlocking frictional particles and that the regimes of soil behavior depend in a major way on its density and effective pressure.

In the critical state view, liquefaction occurs when soil is on the dry side of critical states, near zero effective stress, and in the presence of high hydraulic gradients. In this view liquefaction is one of a group of phenomena; including piping, boiling, and fluidization; with pipes and channels and hydraulic fractures, internal erosion and void migration. This study uses the critical state framework to put forward a consistent methodology to characterize the different regimes of fine-grained soil behavior under earthquake loads.

The central piece of the proposed characterization of soil behavior is the stability diagram shown in Figure 4-1, where $\eta = q / p'$ and $LI_5 = LI + 0.5 \log (p'/5)$ (Equation 3-7). Thus, this diagram captures the effects of soil plasticity through LI, confinement through mean normal effective stress p', and shear stress q through the stress ratio η. The three regions of behavior; fracture, fault, and fold/yield were identified using the data from Weald clay (Equations 4-1a-c). Soils at rest are stable, and therefore plot below the $\eta = 1$ line. Additionally, some of the data (circled in red in Figure 4-2a) from Taiwan and Turkey plot on the negative side of LI_5 axis. These soils are prone to fracture and would result in unstable failures when disturbed by earthquake or other causes. Soils that lie outside of the cam clay region remain stable due to interparticle bonding, which can be broken under earthquake loads and may lead to unstable failures. Soils become susceptible to liquefaction ("unsafe") when they shift above the $\eta = 1$ line in the fracture zone ($LI_5 \leq 0.4$), or if they plot outside of the cam clay region (Figure 4-1).

During an earthquake soils undergo shear stresses as well as a rise in pore pressure. Therefore, both q and the effective stress p′ change, resulting in a shift of the shear stress ratio η. These changes were determined as a function of earthquake magnitude, peak ground acceleration a_{max}, and confinement stress using appropriate equations.

The proposed characterization of the regions of soil behavior was used to examine the liquefaction susceptibility of fine-grained soils from China, Taiwan, and Turkey. From the field data of these soils, the liquidity index and the mean effective confining stress were determined. These values were used to determine the equivalent LI_5 values. The vertical effective stress was determined at the different depths and used to calculate the horizontal effective stress at rest. These values were in turn used to calculate the shear stress ratio η and the LI_5 and η values plotted on the stability diagram to determine the nature of stability of the soils. The shifts of these points under various magnitudes of a_{max} were determined as shown in Figures 4-6 a, b, and c.

The shift in stress ratio η is affected by peak ground acceleration of the applied earthquake and depth of the in-situ soil. The analyses show that the smaller the upward shift in η and the smaller the shift in LI_5, the more likely the soil is to remain safe from liquefaction. A higher a_{max} value causes an increase in η. A greater depth below ground surface results in a decrease in η. A depth of about 15 meters is the threshold for liquefaction safety; an earthquake with $a_{max} > 0.9g$, a force yet to be recorded, would be required for a significant shift in η below 15 meters. Additionally, a larger magnitude earthquake causes a larger leftward shift in LI_5 on the (η, LI_5) plot, which puts a soil closer to liquefaction danger.

When compared to the critical state framework approach, the Chinese criteria are unconservative in predicting liquefaction potential. Using the field studies of fine-grained

liquefaction sites, the Chinese criteria predicts only 13.2% of the soils to be liquefiable, whereas the critical state approach identifies 68.9% of the data set as potentially liquefiable at a relatively low peak ground acceleration of 0.2g. The critical state framework provides a broader characterization with the inclusion of depth and earthquake load in addition to soil plasticity characteristics.

Natural cementation and interparticle bonding enables the soil at rest to exist in conditions outside the LI_5 boundary limit of about 1.9 given by the cam clay model. However, such soils are sensitive to disturbance and in danger of sudden instability and liquefaction when a sudden load such as an earthquake breaks the bonds and the structure collapses.

Recommendations for Further Study

The strength of an earthquake affects liquefaction susceptibility. As seen in Figure 4-3, the data shows a strong correlation between greater changes in shear stress and a greater likelihood of liquefaction. Higher shear stresses are a result of higher peak ground accelerations. Earthquake magnitude is a familiar measure of an earthquake's 'size.' A quantifiable correlation between earthquake magnitude and liquefaction potential would be an asset to determining risk, using the hypocentral distance to the site to determine the most probable peak ground acceleration in the manner of probabilistic seismic hazard analysis (PSHA).

A soil will remain liquefied as long as it is under cyclic load. Arguably, longer periods of continuous liquefaction lead to more damage, up to a theoretical limit of maximum damage for a site. Earthquake duration, then, could be included when assessing seismic risk for a site that has been determined to be potentially liquefiable. This is important because more earthquake cycles

generally indicate longer durations; therefore sites that are more likely to liquefy could be susceptible to higher damage when that liquefaction occurs.

The fold-fault-fracture failure surface of critical state soil mechanics is based on the characteristics of Weald clay, the material used by Schofield at Cambridge University to develop the critical state theory. While it is a good model for a broad range of clays, soil stress states that plot near the line may be inaccurately classified as 'safe' or 'unsafe' due to discrepancies in the actual soil qualities from Weald clay characteristics. Ideally, a failure surface would be developed for each type of clay, or for groups of similar clays, to be able to more accurately predict liquefaction potential in borderline situations. Additionally, specific surfaces for silts should eventually be developed for similar use.

REFERENCES

Andrews, D.C.A. and Martin, G.R. (2000). "Criteria for liquefaction of silty soils." *Proc., 12th World Conference on Earthquake Engineering*, NZ Society for Earthquake Engineering, Upper Hutt, New Zealand, Paper No. 0312.

Ansal, A.M., and Erken, A. (1989). "Undrained behavior of clay under cyclic shear stresses." *Journal of Geotechnical Engineering*, 115(7), 968-983.

Boulanger, R.W. and Idriss, I.M. (2006). "Liquefaction susceptibility criteria for silts and clays." *Journal of Geotechnical and Geoenvironmental Engineering*, 132(11), 1413-1426.

Bray, J.D. and Sancio, R.B. (2006). "Assessment of the liquefaction susceptibility of fine-grained soils." *Journal of Geotechnical and Geoenvironmental Engineering*, 132(9), 1165-1177.

Bray, J.D., Sancio, R.B., Riemer, M., and Durgunoglu, H.T. (2004). "Liquefaction susceptibility of fine-grained soils." *Proc., Joint Conference, the 11th International Conference on Soil Dynamics and Earthquake Engineering (SDEE), the 3rd International Conference on Earthquake Geotechnical Engineering (ICEGE)*, Berkeley, Ca., 655-662.

Casagrande, A. (1975). ''Liquefaction and cyclic deformation of sands—a critical review.'' *Proc., 5th Pan-American Conference. on Soil Mechanics and Foundation Engineering*, Buenos Aires, Argentina.

Holzer, T.L., Bennett, M.J., Ponti, D.J., and Tinsley, J.C., III (1999). "Liquefaction and soil failure during 1994 Northridge earthquake." *Journal of Geotechnical and Geoenvironmental Engineering*, 125(6), 438-452.

Kramer, Steven L. (1996). *Geotechnical Earthquake Engineering.* Prentice Hall, New Jersey.

Lawrence, D.M., (1980), Some properties associated with Kaolinite soils, Ph. D. Thesis, Gonville and Caius College, Cambridge University, Cambridge, UK.

Muhunthan, B. and Pillai, V.S. (2008). "Teton Dam, USA: Uncovering the crucial aspect of its failure." *Proceedings of the Institution of Civil Engineers*, 161(CE6), 35-40.

Muhunthan, B. and Pillai, V.S. (2009). "Response of the Authors to the Discussion by Dr. J. S. Younger regarding 'Teton Dam, USA: Uncovering the crucial aspect of its failure.'" *Proceedings of the Institution of Civil Engineers*, in press.

Muhunthan, B. and Schofield, A.N. (2000). "Liquefaction and dam failures." *Proceedings of GeoDenver 2000*, Denver, Co.

Papathanassiou, G. (2008). "LPI-based approach for calibrating the severity of liquefaction-induced failures and for assessing the probability of liquefaction surface evidence." *Engineering Geology*, 96, 94-104.

Perlea, V.G. (2000). "Liquefaction of coheseive soils." *Proc., Soil Dynamics and Liquefaction 2000, Geotechnical Special Publication 107*, R.Y.S. Pak and J. Yamamuro, eds, ASCE, Reston, Va., 58-76.

Pillai, V.S., Muhunthan, B., and Sasiharan, S. (2004). "The failure of the Teton Dam: a new theory based on state based soil mechanics." *Proceedings of 5th International Conference on Case Histories in Geotechnical Engineering* (CD-ROM).

Polito, C. (2001). "Plasticity based liquefaction criteria." *Proc., 4th International Conference On Recent Advances In Geotechnical Earthquake Engineering and Soil Dynamics,* University of Missouri-Rolla, Rolla, Mo., Paper No. 1.33.

Rauch, A.F. (1997). "EPOLLS: An Empirical Method for Predicting Surface Displacements Due to Liquefaction-Induced Lateral Spreading in Earthquakes," thesis, presented to Virginia Polytechnic Institute and State University at Blacksburg, Va., in partial fulfillment of the requirements for the degree of Doctor of Philosophy.

Roscoe, K.H., Schofield, A.N., and Wroth, C.P. (1958). "On the yielding of soils." *Géotechnique*, 8(1), 22-53.

Sangrey, D.A. (1972). "Naturally cemented sensitive soils." *Géotechnique*, 22(1), 139-152.

Sariosseiri, F. and Muhunthan, B. (2008). "Effect of cement treatment on geotechnical properties of some Washington soils." *Engineering Geology*, in press.

Schofield, A.N. (1980). Cambridge geotechnical centrifuge operations, 20th Rankine Lecture, *Géotechnique*, 30(3), 227-268.

Scofield, A.N. (2005). *Disturbed Soil Properties and Geotechnical Design.* Thomas Telford, London.

Schofield, A.N. and Wroth P. (1968). *Critical State Soil Mechanics*. McGraw-Hill, New York.

Seed, H.B. and Idriss, I.M. (1982). *Ground motions and soil liquefaction during earthquakes*, Earthquake Engineering Research Institute, Berkeley, Calif.

Wang, W.S. (1979). *Some findings in soil liquefaction*, Water Conservancy and Hydroelectric Power Scientific Research Institute, Beijing.

Youd, T.L., et al. (2001). "Liquefaction resistance of soils: Summary report from the 1996 NCEER and 1998 NCEER/NSF workshops on evaluation lf liquefaction resistance of soils." *Journal of Geotechnical and Geoenvironmental Engineering*, 127(10), 817-833.